Dalton Transactions

Accepted Manuscript

This article can be cited before page numbers have been issued, to do this please use: H. Pang, C. Wei, C. Cheng, Y. Y. Cheng, Y. Wang, Y. Z. Xu and W. M. Du, *Dalton Trans.*, 2015, DOI: 10.1039/C5DT02724A.

This is an *Accepted Manuscript*, which has been through the Royal Society of Chemistry peer review process and has been accepted for publication.

Accepted Manuscripts are published online shortly after acceptance, before technical editing, formatting and proof reading. Using this free service, authors can make their results available to the community, in citable form, before we publish the edited article. We will replace this *Accepted Manuscript* with the edited and formatted *Advance Article* as soon as it is available.

You can find more information about *Accepted Manuscripts* in the Information for Authors.

Please note that technical editing may introduce minor changes to the text and/or graphics, which may alter content. The journal's standard Terms & Conditions and the Ethical guidelines still apply. In no event shall the Royal Society of Chemistry be held responsible for any errors or omissions in this *Accepted Manuscript* or any consequences arising from the use of any information it contains.

ROYAL SOCIETY OF CHEMISTRY

www.rsc.org/dalton

Journal Name

View Article Online
DOI: 10.1039/C5DT02724A

ARTICLE

Comparison of NiS_2 and α-NiS hollow spheres for supercapacitors, non-enzymatic glucose sensors and water treatment

Received 00th January 20xx,
Accepted 00th January 20xx

DOI: 10.1039/x0xx00000x

www.rsc.org/

Chengzhen Wei,*[a] Cheng Cheng,[a] Yanyan Cheng, [a] Yan Wang, [a] Yazhou Xu, [a] Weimin Du [a] and Huan Pang* [a,b]

NiS_2 hollow spheres are successfully prepared by one-step template free method. Meanwhile, α-NiS hollow spheres can also be synthesized via the calcination of pre-obtained NiS_2 hollow spheres under 400 °C for 1 h in air. The electrochemical performances of the as-prepared NiS_2 and α-NiS hollow spheres products are evaluated. When used for supercapacitors, compared with NiS_2 hollow spheres, the α-NiS hollow spheres electrode shows a large specific capacitance of 717.3 F g^{-1} at 0.6 A g^{-1} and a good cycle life. Furthermore, NiS_2 and α-NiS hollow spheres are successfully applied to fabricate non-enzymatic glucose sensors. Especially, the α-NiS hollow spheres exhibits good catalytic activity for the oxidation of glucose, a fast amperometric response time of less than 5 s, and the detection limit is estimated to be 0.08 μM. More importantly, compared with other normally co-existing interfering species, such as ascorbic acid, uric acid and dopamine, the electrode modified with α-NiS hollow spheres shows good selectivity. Moreover, the α-NiS hollow spheres also present good capacity to remove Congo red organic pollutants from waste water by their surface adsorption ability.

1. Introduction

In recent years, the synthesis of micro/nano structured materials with controlled size, shape, composition and internal structure have received tremendous interest for achieving novel morphology-dependent chemical-physical properties.[1-6] In particular, hollow nanostructures materials with interior voids, low density, and surface permeability has potential applications in many fields, such as energy storage, catalysis, sensors, drug delivery, and water treatment.[7-12] In general, hollow materials are prepared via template directed approaches. However, this kind of synthetic route is quite costly, tedious, and low yield. Moreover, template contamination mostly decreased the activity of synthesized materials.[13-16] To overcome these problems, a number of template-free routes have been devised for preparing hollow materials.[17-19] Despite the intense efforts have been dedicated, it is still of huge challenge to develop a facile, reliable, and scalable route for the rational synthesis of hollow structured materials.

Electrochemical energy storage provides a promising technology for portable energy supplies in fields such as electric vehicles and mobile electronic products. Supercapacitors that store energy have recently received considerable attention because of their high power density, excellent charge-discharge characteristics, long cycling life and good safety.[20, 21] Up to date, various materials, including carbonaceous materials, transition metal oxides/hydroxides and hybrid composite, have been widely studied as electrodes for supercapacitors.[22-25] Compared to carbonaceous materials, transition-metal oxides show larger electrochemical capacitances and energy densities as they can provide variable oxidation states for efficient redox charge transfer. In particular, supercapacitors based on RuO_2 have exhibited a high specific capacitance and excellent reversibility. However, the high cost of Ru-based materials makes this material unsuitable for practical applications.[26] Hence, searching for alternative electrode materials with good capacitive properties becomes important. Semiconducting transition metal sulfides, such as MoS_2, ZnS, CuS, Ni_7S_6, Co_3S_4, CoS_2 and NiS_2, etc. are reported to be viable

[a] College of Chemistry and Chemical Engineering, Anyang Normal University, Anyang, 455000 Henan, P. R. China.
E-mail:chengzhenweichem@126.com, huanpangchem@hotmail.com.
[b] College of Chemistry and Chemical Engineering, Yangzhou University, Yangzhou, 225002, Jiangsu, P. R. China.

View Article Online
DOI: 10.1039/C5DT02734J

candidates.[27-33] Among them, Ni-based sulfides materials are of particular interest owing to their high theoretical specific capacitance and low cost.[34]

The development of highly sensitive, low-cost, reliable, fast glucose sensors is becoming gradually important because of their applications in clinical diagnostics, biotechnology and food industry.[35] The conventional glucose sensors involve the use of glucose oxidase (GOD). However, these GOD-based biosensor approaches suffer greatly from the influences of various environmental factors such as temperature, humidity, pH value, organic reagents, and toxic chemicals, which limit their wide applications.[36] To solve this problem, the non-enzymatic glucose biosensors have been pursued increasingly. The recent researches exhibit that many nano/microstructured materials have been successfully used for the construction of non-enzymatic glucose sensors, such as Ni, Cu, NiO, NiS and CuS materials, etc.[37-41] Furthermore, these nano/microstructured materials also exhibit good performance for the detection of glucose in the absence of enzyme. However, there are few reports on the fabrication of non-enzymatic glucose detectors based on Ni-based sulfides micro/nanomaterials.

Herein, NiS_2 hollow spheres were successfully prepared via a simple and general hydrothermal synthetic route. Interestingly, α-NiS hollow spheres could also be synthesized by the calcination of NiS_2 hollow spheres under 400 °C for 1 h in air, which inspired us to study the performance of NiS_2 and α-NiS hollow spheres under the same conditions. The electrochemical performances of the NiS_2 and α-NiS hollow spheres were evaluated. Especially, α-NiS hollow spheres showed a large specific capacitance of 717.3 F g^{-1} at 0.60 A g^{-1} and a good cycle life. More importantly, the NiS_2 and α-NiS hollow spheres were also tested as electrochemical catalysts. It is found that α-NiS hollow spheres exhibited a high selectivity, high sensitivity and low detection limit toward the oxidation of glucose. Moreover, the as-prepared α-NiS hollow spheres also displayed a good ability to remove the organic pollutant Congo red from water compared with that of NiS_2 hollow spheres. These results demonstrate that α-NiS hollow spheres hold great potential applications in supercapacitors, enzyme-free determination of glucose and waste water treatment.

2. Experimental

2.1 Synthesis of NiS_2 and α-NiS hollow spheres

The typical procedure for NiS_2 and α-NiS hollow spheres is as follows[6]: 0.5 mmol $Ni(NO_3)_2 \cdot 6H_2O$ was dissolved in 20 mL distilled water at room temperature. Then, L-cysteine (2.0 mmol) and urea (0.5 mmol) were added to the above mentioned solution under an ultrasonic treatment. The homogeneous solution was transferred into a 35 mL Teflon-lined autoclave. Then the autoclave was sealed and maintained at 140 °C for 24 h, and allowed to cool to room temperature naturally. The resulting NiS_2 hollow spheres precipitate was repeatedly washed with ethanol several times, then dried at 50 °C for 12 h. α-NiS hollow spheres were obtained after calcination of the as-prepared NiS_2 hollow spheres in air at 400 °C for 1 h.

2.2 Fabrication of the three-electrode supercapacitors

The working electrode was prepared by mixing the electroactive material (NiS_2 or α-NiS), acetylene black, and polytetrafluoroethylene (PTFE) with a weight ratio of 85:10:5. The mixture was then pressed onto a nickel grid (1 cm^{-2}). The electrochemical performance of the NiS_2 and α-NiS sample were evaluated by using a three-electrode cell with Pt foil as the counter electrode and a saturated calomel electrode (SCE) as the reference electrode in 3.0 M KOH aqueous solution.

2.3 Fabrication of the glucose sensor

The glassy carbon (GC) electrodes were carefully polished with alumina slurry, rinsed thoroughly with distilled water and ethanol, and then dried at room temperature. To fabricate NiS_2 or α-NiS containing GC electrodes, an aqueous dispersion of NiS_2 or α-NiS (1.0 mg mL^{-1}) was prepared and 8 μL of the suspension was cast on the surface of the GC electrodes. Subsequently, the solvent was allowed to evaporate at room temperature, leaving the as-prepared NiS_2 or α-NiS material immobilized onto the GC electrode surface.

2.4 Removal of Congo red

60 mg of the as-prepared NiS_2 and α-NiS hollow spheres powder were mixed with 150 mL of aqueous solution of Congo red with a concentration of 100 mg L^{-1} in a beaker, respectively. The suspension was stirred at room temperature. At given time intervals, a series of aqueous solution were taken out and separated through centrifugation (10000 rpm min^{-1}). The supernatant solutions were analyzed with UV-vis spectroscopy (Hitachi U-3900) to determine the concentrations of Congo red in solution.

2.5 Characterization

X-ray diffraction (XRD) patterns were recorded on a Rigaku-Ultima III with Cu-K_α radiation (λ=1.5418 Å). The morphologies of the as-prepared samples were observed using a field-emission scanning electron microscope (FESEM, JEOL JSM-6701F) operated at an acceleration voltage of 3.0 kV. Transmission electron microscopy (TEM) and high-resolution transmission electron microscopy (HRTEM) were taken on the JEOL JEM-2100 microscope at an acceleration voltage of 200 kV. The nitrogen adsorption and desorption isotherms were measured on a Micromimetrics ASAP2020 physisorption analyzer. The electrochemical supercapacitor measurements were measured by using an electrochemical analyzer system CHI660D (Chenhua, Shanghai, China).

3. Results and discussion

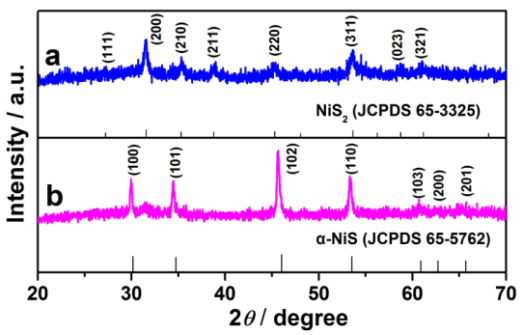

Fig. 1 XRD patterns of as-synthesized samples: (a) NiS_2; (b) α-NiS.

DOI: 10.1039/C5DT02724A

Typical XRD patterns of the as-synthesized samples are shown in Fig. 1. The obtained diffraction peaks are labeled in Fig. 1a and b agreed well with the standard patterns of the NiS_2 (JCPDS card No. 65-3325) and α-NiS (JCPDS card No. 65-5762). No peaks of any impurity phase could be observed from these patterns, indicating the high purity of the as-synthesized NiS_2 and α-NiS products.

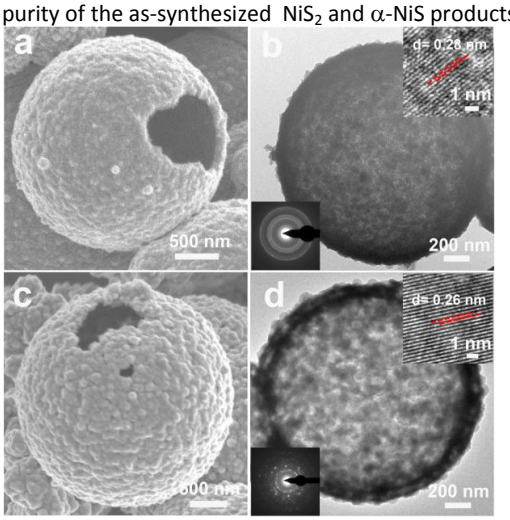

Fig. 2 (a, b) SEM and TEM images of the NiS_2; (c, d) SEM and TEM images of the α-NiS. The inset in b and d show SAED patterns and HRTEM images of the NiS_2 and α-NiS, respectively.

The morphologies and structures of the NiS_2 and α-NiS products were characterized by field emission scanning electron microscopy (FESEM) and transmission electron microscopy (TEM). Panoramic FESEM image of NiS_2 exhibited in Fig. S1a clearly presents that the product is entirely composed of large amounts of spherical structures. Several broken nanostructures in Fig. S1a obviously reveal the hollow nature of the as-prepared NiS_2 spheres. Close-up FESEM micrograph of an individual hollow NiS_2 spheres (Fig. 2a) shows that the NiS_2 hollow spheres possess quite rough surfaces, which are built up from numerous densely packed nanoparticles. The hollow interior of NiS_2 spheres could also be clearly identified by the sharp contrast between the dark edge and the pale center in the TEM image of an individual NiS_2 sphere (Fig. 2b). Selected-area electron diffraction (SAED) pattern (inset in the Fig. 2b) shows that NiS_2 hollow spheres are composed of high crystalline nanocrystals. The lattice fringes in high-resolution TEM (HRTEM) image (inset in the Fig. 2b) shows a spacing of 0.28 nm, corresponding to the (200) planes of the NiS_2. After being annealed at 400 °C in air for 1 h, the as-prepared NiS_2 hollow spheres are fully converted to α-NiS (Fig. 1b). It is interesting and exciting that α-NiS remains the hollow sphere structure (Fig. S1b and Fig. 2c). The corresponding TEM image (Fig. 2d) confirms the formation of hollow structure. A representative high-resolution transmission electron microscopy image of the α-NiS shows a typical lattice fringe spacing of 0.26 nm, corresponding to the (101) plane of the α-NiS. The SAED pattern shows that the α-NiS hollow sphere is polycrystalline (inset of Fig. 2d). To illustrate the spatial distribution of Ni and S elements in the NiS_2 and α-NiS hollow spheres, the EDS elemental mapping is performed on hollow spheres under SEM observation. The EDS elemental mapping results demonstrate that the NiS_2 and α-NiS hollow spheres are uniform distribution of Ni and S elements (Fig. S2).

In our paper, NiS_2 and α-NiS hollow spheres were prepared via the previous reported methods, in which the NiS_2 hollow spheres were formed via the Ostwald ripening process.[6] In the preparation system, urea plays an important role for the formation of hollow structured NiS_2. Without adding urea, irregular nanoparticles were obtained (Fig. S3). We believed that L-cysteine is not only provided S source but also can be capped by Ni ions due to the coordination of functional groups in the L-cysteine molecules. Meanwhile, urea can be used to provide an alkaline environment, after reaction for 24 h under 140 °C, the NiS_2 hollow spheres were obtained under the hydrothermal conditions. In addition, we also found out that the NiS_2 hollow spheres can be obtained under the 160 °C and 200 °C (Fig. S4), which demonstrates that the reaction temperature has no effect on the preparation of NiS_2 hollow spheres.

The surface area and pore size distribution of the NiS_2 and α-NiS with hollow interiors were further determined by nitrogen adsorption-desorption measurements. As revealed by the nitrogen adsorption-desorption measurement (Fig. 3), the BET specific surface areas of the NiS_2 and α-NiS hollow spheres are 15.3 and 32.2 $m^2 g^{-1}$, respectively. The pore sizes of NiS_2 hollow spheres are about 2.8 nm, while the α-NiS hollow spheres contain two types of mesopores (ca. 2.4 and 3.0 nm).

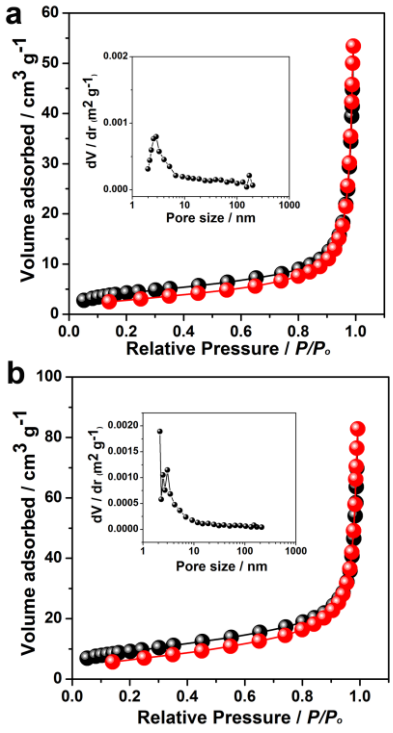

Fig. 3 Nitrogen adsorption-desorption isotherm (with the BJH pore size distribution plot in the inset) of the as-synthesized samples: (a) NiS_2; (b) α-NiS.

In particular, hollow sphere structures have several advantages in electrochemical, catalysis and adsorption property. The hollow interior space effectively reduces the mass weight and enhances the spatial dispersion, which results in not only high surface area but also better mass transportation.[42-45] In order to explore the

advantages of the NiS_2 and α-NiS hollow spheres, the as prepared products were firstly evaluated as electrochemical materials to study their electrochemical properties. Cyclic voltammetry (CV) measurements were conducted on the NiS_2 and α-NiS electrodes in 3.0 M KOH solution. Fig. 4a and b show the CV curves of the NiS_2 and α-NiS electrode at different scan rates. The shapes of the CV reveal that the capacitance characteristic is very different from that of traditional electric double-layer capacitance, indicating that the capacity mainly results from pseudocapacitive capacitance.[46, 47] The mechanisms of the NiS_2 and α-NiS supercapacitors occur like below:

$$NiS_2 + H_2O + 1/2\ O_2 \longrightarrow Ni(OH)_2 + 2S \quad (1)$$

$$NiS + H_2O + 1/2\ O_2 \longrightarrow Ni(OH)_2 + 2S \quad (2)$$

$$Ni(OH)_2 + OH^- \Longleftrightarrow NiOOH + H_2O + e^{-1} \quad (3)$$

A pair of redox peaks can be observed (Fig. 4a and b), which is corresponding to the reversible conversion between $Ni(OH)_2$ and NiOOH.[34] Fig. S5 shows CV curves of NiS_2 and α-NiS hollow sphere electrodes at 50 mV s^{-1} in 3.0 M KOH electrolyte. Interestingly, the CV curve of α-NiS electrode has a bigger surrounded area compared to that of the NiS_2 electrode, suggesting that the capacitance of α-NiS electrode might be larger than that of the NiS_2 electrode.

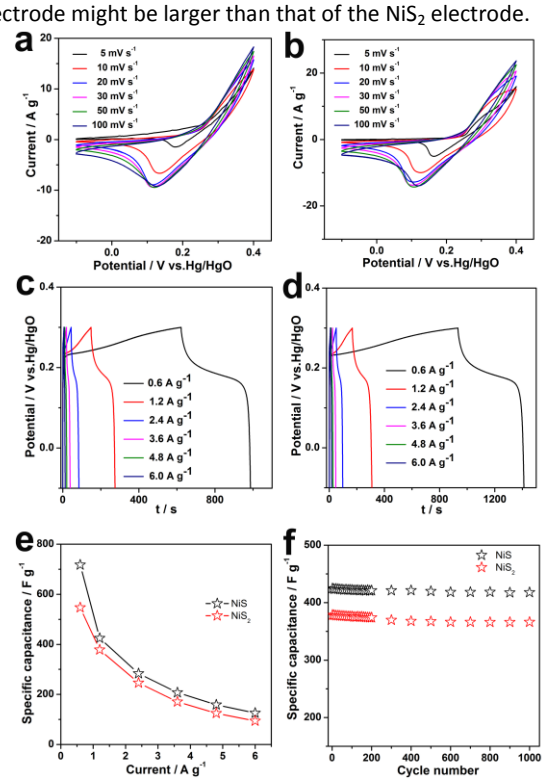

Fig. 4 (a, b) CV curves of NiS_2 and α-NiS hollow sphere electrodes at a scan rate of 5 to 100 mV s^{-1}; (c, d) The galvanostatic charge-discharge curves of NiS_2 and α-NiS hollow sphere electrodes at different current densities in 3.0 M KOH electrolyte; (e) The specific capacitances calculated from the discharging curves at different current densities; and (f) Plots of the specific capacitance as a function of cycle number at a current density of 1.2 A g^{-1}.

To further evaluate the electrochemical properties of the as-prepared NiS_2 and α-NiS hollow sphere, galvanostatic charging and discharging of NiS_2 and α-NiS electrodes were performed in 3.0 M KOH solution. The specific capacitance of the electrode can be estimated by the following formula:[48, 49]

$$C=(I\Delta t)/(m\Delta V) \quad (4)$$

Where C (F g^{-1}) is the specific capacitance, I (A) is the discharge current, Δt is the time for discharge duration, m (g) is the mass of the active material within the electrode, ΔV is the voltage interval of the discharge.

The specific capacitances were calculated from the galvanostatic discharge (Fig. 4c and d) curves at current densities of 0.6-6.0 A $g^{-1}$are shown in Fig. 4e. The specific capacitances are 547.2 F g^{-1} (NiS_2) and 717.3 F g^{-1} (α-NiS) at 0.6 A g^{-1} in 3.0 M KOH solution. At a high current density of 6.0 A g^{-1}, the specific capacitance of α-NiS was 125.4 F g^{-1}, while that of NiS_2 was reduced to 93.8 F g^{-1}. Moreover, compared with other electrode materials, the specific capacitance of α-NiS hollow sphere electrode is significantly better than some electrode materials, such as MoS_2 (1 A g^{-1}, 168 F g^{-1}),[50] β-NiS (0.6 A g^{-1}, 501.5 F g^{-1}),[40] Co-Ni-Mn oxide (0.5 A g^{-1}, 578 F g^{-1}).[51] However, the specific capacitance of the α-NiS hollow sphere electrode is not greater than that of some metal sulfides materials.[29, 52] Electrochemical stability is another important parameter to evaluate the active materials for supercapacitor applications. Fig. 4f presents the cycling performance of the NiS_2 and α-NiS electrode within 1000 cycles at the current density of 1.2 A g^{-1}. After subsequent 1000 cycles, there is only a small (1.5 %) loss of capacitance for α-NiS electrode. It is notable that the retention ratio of the NiS_2 electrode is approximately 96.5 %. This high specific capacitance of α-NiS can mainly be attributed to the high surface area (α-NiS: 32.2 m^2 g^{-1}, NiS_2: 15.3 m^2 g^{-1}) and hollow nanostructure, which provide effective diffusion channels for the electrolyte ions. More importantly, compared with the NiS_2 crystal structure at the atomic scale, there are more Ni atoms exposed on the surface of α-NiS than the NiS_2 (Fig. S6 and S7), which is also beneficial for Faradic reactions during the charge-discharge process.[40, 53, 54, 55]

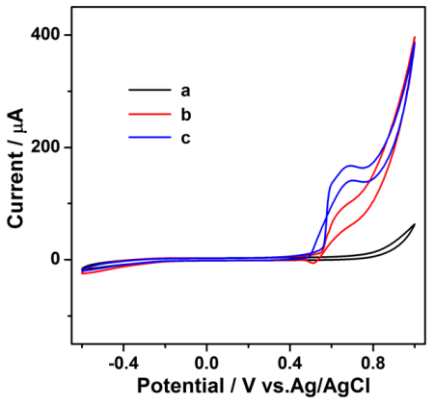

Fig. 5 Cyclic voltammograms of the bare GC electrode (a); NiS_2-GC electrode (b); and α-NiS-GC electrode (c) in 0.1M NaOH with 5 mM glucose at a scan rate of 50 mV s^{-1}.

The development of nonenzymatic glucose sensors with high sensitivity, fast response, and good stability has become one of the most attractive subjects of investigation in electrochemistry due to the practical applications. Transition metal sulfides materials by

virtue of low cost, good electrocatalytic properties are of particular interest, which make them suitable for the electrochemical sensors.[40, 41, 56] The possible mechanism for oxidation of glucose by the NiS_2 and α-NiS hollow spheres materials could be represented by the following reactions: First, Ni^{2+} could be electro-oxidized to Ni^{3+} in alkaline solution, where the release of electron resulted in the formation of oxidation peak current. Then, glucose could be oxidized to gluconic acid by Ni^{3+}, which was deoxidized to Ni^{2+}at the same time.[35] To demonstrate the sensing application of the NiS_2 and α-NiS hollow spheres, nonenzymatic glucose sensor was constructed by deposition of the aqueous dispersion of NiS_2 or α-NiS hollow spheres on a GC electrode surface. Fig. 5 presents the CVs of bare GC electrode and NiS_2 or α-NiS hollow spheres modified GC electrode in 0.1 M NaOH solution in the presence of 5.0 mM glucose at a scan rate of 50 mV s^{-1}. It is found that the bare GC electrode shows no obvious oxidation peak in the presence of glucose, demonstrating that the response of bare GC electrode toward the oxidation of glucose is pretty weak (Fig. 5a). In contrast, upon the addition of 5.0 M glucose, a more dramatic increase can be found after the GC electrode was modified with NiS_2 or α-NiS (Fig. 5b and c), indicating good electrocatalytic activity in response to glucose. Furthermore, the α-NiS /GC electrode shows a much stronger signal than that of NiS_2/GC electrode.

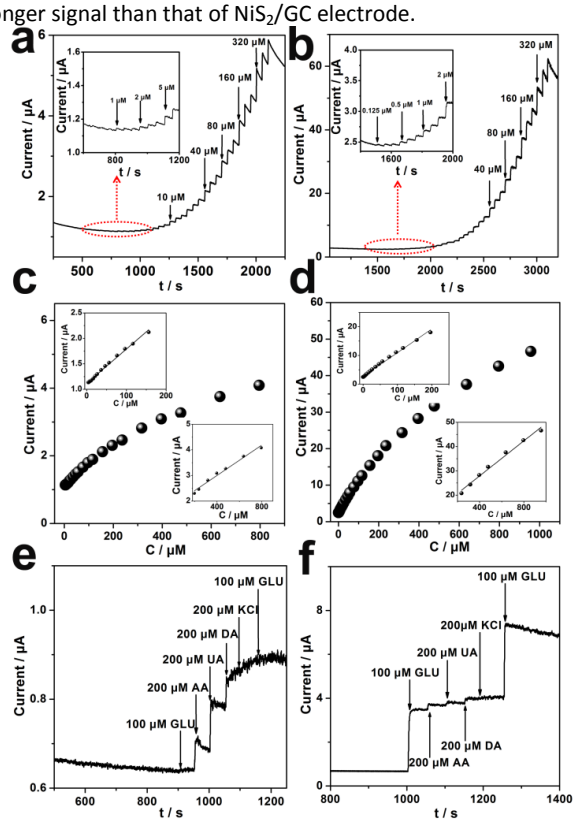

Fig. 6 Current-time response at a potential of 0.60 V upon successive injection of different amounts of glucose into 0.1M NaOH with stirring for (a) NiS_2/GC electrode and (b) α-NiS /GC electrode; (c, d) Plots of the electrocatalytic current of glucose versus glucose concentration for (c) NiS_2/GC electrode and (d) α-NiS /GC electrode; (e, f) Amperometric response of modified electrodes with successive addition of glucose, AA, UA, DA, KCl, and glucose in 0.1 M NaOH solution for (e) NiS_2/GC electrode and (f) α-NiS /GC electrode.

Fig. 6a and b show typical amperometric response curves of different concentrations of glucose at the NiS_2/GC electrode and α-NiS/GC electrode, respectively. The proposed sensors rapidly responded to the changes of glucose concentration and achieved steady-state current within 5s, demonstrating the good electrocatalytic ability of the NiS_2/GC electrode and α-NiS/GC electrode for glucose oxidation. To our surprise, it is noted that the current signals increase more rapidly with a higher sensitivity for the α-NiS/GC electrode compared with the NiS_2/GC electrode. The calibration curves for the NiS_2/GC electrode and α-NiS/GC electrode sensors are shown in Fig. 6c and d. The NiS_2/GC electrode sensor displays a linear range from 4.0 μM to 0.15 mM glucose (R= 0.9936), a sensitivity of 5 μA mM^{-1} and a detection limit of 0.45 μM (S/N = 3), whereas the α-NiS/GC electrode sensor displays the glucose detection concentration range of 0.125 μM-0.2 mM (R=0.9969), and the calculated sensitivity is 80 μA mM^{-1}. The limit of detection is calculated to be as low as 0.08 μM (S/N = 3). Furthermore, the α-NiS/GC electrode sensor was also used for detection of glucose with a relatively wide concentrations ranging from 0.24 mM to 1.0 mM. The performance of the as-prepared α-NiS/GC electrode sensor was also compared to some existing non-enzymatic sensors. The detection limits of some previously reported materials are lower than that of our system, such as NiO/C nanoblets (9.12 nM),[57] $MnCo_2O_4$ nanofibers (0.01 μM) and CuO-NiO microfibers (1 nM).[58, 59] However, the detection limit of glucose for the α-NiS/GC electrode sensor is better than those of many non-enzymatic sensors, such as β-NiS (20 μM),[40] CuS (0.25 μM),[41] NiO (0.23 μM),[57] $Ni(OH)_2$ hollow spheres (0.1 μM),[60] Cu-NiO (0.5 μM),[61] $NaCoPO_4$-Co_3O_4 hollow microspheres (0.125 μM) and Nitrogen-doped carbon-copper nanohybrids (5 μM).[62, 63] The results confirm that α-NiS hollow sphere can be a promising functional material for the electroanalytical detection of glucose. The excellent sensing properties of the as-fabricated α-NiS/GC glucose sensor can be attributed to the improved electrochemical and electrocatalytic performances of α-NiS/GC electrode. Firstly, the electro-oxidation of glucose at the modified electrode can be catalyzed by α-NiS hollow sphere that was directly immobilized onto the GC electrode surface. Secondly, the conductive α-NiS hollow sphere is able to keep electrical connection between the hollow spheres and electrode, and thus facilitates the charge transfer in those interfaces. That is to say, direct electron transfer can be achieved between α-NiS hollow sphere and electrode, which is an important reason of fast and sensitive catalytic performances. Thirdly, more Ni atoms are exposed on the surface of α-NiS hollow spheres (Fig. S7), the oxidation of glucose by α-NiS hollow spheres could occur easily. Finally, the hollow structure of α-NiS ensures that the glucose can enter into the interior of the α-NiS and thus shorten the diffusion distance for glucose to access the electrode surface, resulting in an improved signal-to-noise ratio and faster response time.[57, 64, 65]

One of the most important performance parameters for a non-enzymatic sensor is the ability to discriminate interfering species from the target analyte. It is well known that some easily oxidative species such as ascorbic acid (AA), uric acid (UA), dopamine (DA) usually co-exist with glucose and can cause interfering signals.

Therefore, the electrochemical response of the interfering species was also examined at the NiS_2/GC electrode and α-NiS/GC electrode. The results showed that addition of 200 μM AA, DA, and UA induces the increasing the current of NiS_2/GC electrode, the intensity increased is much stronger than that of glucose (Fig. 6e). It indicates that NiS_2/GC electrode shows not good selectivity toward AA, DA, and UA. As shown in Fig. 6f, although the addition of 200 μM AA, DA, and UA also induces the increasing the current of α-NiS/GC electrode, these interfering species produced negligible current responses compared to glucose, revealing that the non-enzymatic α-NiS/GC electrode sensor showed high selectivity for glucose detection. α-NiS/GC electrode sensor shows a much better selectivity than that of NiS_2/GC electrode sensor, which might be explained that the use of α-NiS hollow spheres on the surface of electrodes can modify the mass transport regime, and this alteration can in favorable circumstances facilitate the amperometric discrimination between species. In addition, there are more Ni atoms exposed on the surface of α-NiS hollow spheres compared with NiS_2 hollow spheres (Fig. S6 and S7), which facilitates contacts with glucose in the case of α-NiS hollow spheres. Thus, non-enzymatic α-NiS/GC electrode sensor presented high selectivity for glucose detection compared with NiS_2/GC electrode sensor.[40, 56, 66, 67]

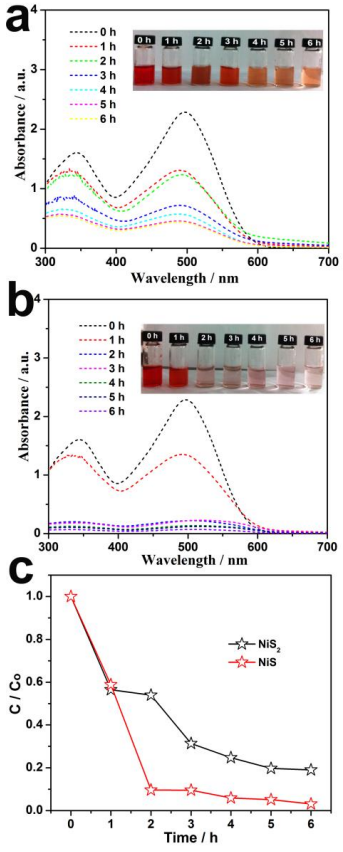

Fig. 7 (a) Absorption spectra of an aqueous solution of 100 mg L^{-1} Congo red in the presence of 60 mg of hollow NiS_2 spheres; (b) absorption spectra of an aqueous solution of 100 mg L^{-1} Congo red in the presence of 60 mg of hollow α-NiS spheres; (c) curves of the adsorption extent of Congo red as a function of contact time for NiS_2 and α-NiS hollow spheres.

The as-synthesized NiS_2 and α-NiS hollow spheres samples were also used to study their possible applications in water purification treatment. Congo red usually used dye in the textile industry, which was chosen as a typical organic water pollutant. Fig. 7a and b show the absorption spectra of an aqueous solution of 100 mg L^{-1} Congo red in the presence of 60 mg of the as synthesized NiS_2 and α-NiS hollow spheres samples. It can be found that α-NiS hollow spheres present good adsorption ability for Congo red dye. Fig. 7c gives curves of the adsorption extent of Congo red as a function of contact time for NiS_2 and α-NiS hollow spheres. It also reveals that α-NiS hollow spheres show better adsorption ability than NiS_2 hollow spheres. IR characterizations of Congo red and the hollow spheres before and after adsorption were carried out to confirm the adsorption of Congo red on the hollow spheres. From the IR spectra shown in Fig. S8, it can be seen that the IR spectrum of NiS_2 and α-NiS hollow spheres show the characteristic peaks of Congo red after the measurement, demonstrating the adsorption of the Congo red on the surface of NiS_2 and α-NiS hollow spheres. The NiS_2 and α-NiS hollow spheres have specific surface areas of 15.3 $m^2 g^{-1}$ and 32.2 $m^2 g^{-1}$, respectively. Therefore, the difference in the removal ability of NiS_2 and α-NiS hollow spheres might result from their different specific surface areas.[68] Although the removal ability of NiS_2 and α-NiS hollow spheres is not better than NiO and FeOOH,[68, 69] these results show that the α-NiS hollow spheres can significantly remove Congo red, which might have application potential in wastewater treatment.

4. Conclusions

In summary, NiS_2 hollow spheres were synthesized by a facile one-step hydrothermal route. Meanwhile, α-NiS hollow spheres could be simply prepared by the calcination of NiS_2 hollow spheres under 400 °C in air. NiS_2 and α-NiS hollow spheres were subsequently evaluated for their comparative electrochemical performances. It is found that the α-NiS hollow spheres electrode shows a better supercapacitor behavior than the NiS_2 hollow sphere electrode. Moreover, non-enzymatic glucose sensors based on the NiS_2 and α-NiS hollow spheres have been successfully developed for the detection of glucose. The amperometric response indicates that the as-prepared α-NiS/GCE electrode sensor has a high sensitivity, low detection limit, and excellent selectivity compared with the NiS_2/GCE electrode sensor. The results show that α-NiS hollow spheres are a promising material for applications in supercapacitors and electroanalysis. In addition, the as-prepared α-NiS hollow spheres display a good adsorption ability to remove the organic pollutant Congo red from water, which makes them have application potentials in water treatment. This work sheds new light on the material design philosophy for transition metal sulfides, especially for potential applications in supercapacitor, electrocatalysts and waste water treatment.

Acknowledgements

This work is supported by the Program for New Century Excellent Talents of the University in China (grant no. **NCET-13-0645**) and National Natural Science Foundation of China (**NSFC-21201010, U1404203**), Program for Innovative Research Team (in Science and

Technology) in University of Henan Province (**14IRTSTHN004**), the Science & Technology Foundation of Henan Province (122102210253, 13A150019,142102210587,14B150001), the China Postdoctoral Science Foundation (2012M521115) and the opening research foundations of the State Key Laboratory of Coordination Chemistry.

Notes and references

1 D. Zhao, Y. Xiao, X. Wang, Q. Gao, M. H. Cao, *Nano Energy,* 2014, **7**, 124.
2 Y. J. Yin, Y. J. Hu, P. Wu, H. Zhang and C. X. Cai, *Chem. Commun.,* 2012, **48**, 2137.
3 P. Liu, Q. L. Hao, X. F. Xia, L. Lu, W. Lei, X. Wang, *J. Phys. Chem. C,* 2015, **119**, 8537.
4 Y. X. Ye, L. Kuai and B. Y. Geng, *J. Mater. Chem.,* 2012, **22**, 19132.
5 X. P. Shen, Q. Liu, Z. Y. Ji, G. X. Zhu, H. Zhou, K. M. Chen, *CrystEngComm,* 2015, DOI:10.1039/C5CE00840A.
6 W. Ma, Y. F. Guo, X. H. Liu, D. Zhang, T. Liu, R. Z. Ma, K. C. Zhou, G. Z. Qiu, *Chem. Eur. J.,* 2013, **19**, 15467.
7 L. F. Shen, L. Yu, X. Y. Yu, X. G. Zhang, X. W. Lou, *Angew. Chem., Int. Ed.*, 2015, **54**, 1868.
8 G. Z. Chen, F. Rosei and D. L. Ma, *Adv. Funct. Mater.*, 2012, **22**, 3914.
9 P. Sun, X. Zhou, C. Wang, K. G. Shimanoe, G. Y. Lu, N. Yamazoe, *J. Mater. Chem. A,* 2014, **2**, 1302.
10 Y. C. Zhu, J. Lei, Y. Tian, *Dalton Trans.,* 2014, **43**, 7275.
11 Z. H. Wei, . E. Xing, X. Zhang, S. Liu, H. H. Yu, P. C. Li, *ACS Appl. Mater. Interfaces,* 2013, **5**, 598.
12 X. H. Xia, Y. Q. Zhang, D. L. Chao, Q. Q. Xiong, Z. X. Fan, X. X. Tong, J. P. Tu, H. Zhang, H. J. Fan, *Energy Environ. Sci.,* 2015, **8**, 1559.
13 F. S. Cai, G. Y. Zhang, J. Chen, X. L. Gou, H. K. Liu, S. X. Dou, *Angew. Chem.,* 2004, **116**, 4308.
14 X. Y. Lai, J. Li, B. A. Korgel, Z. H. Dong, Z. M. Li, F. B. Su, J. Du, D. Wang, *Angew. Chem., Int. Ed.,* 2011, **50**, 2738.
15 Y. Fu, J. M. Song, Y. Q. Zhu and C. B. Cao, *J. Power Sources,* 2014, **262**, 344.
16 M. Huang, Y. X. Zhang, F. Li, L. L. Zhang, R. S. Ruoff, Z. Y. Wen, Q. Liu, *Sci. Rep,* 2014, **4**, 3878.
17 Y. X. Zhou, H. B. Yao, Y. Wang, H. L. Liu, M. R. Gao, P. K. Shen, S. H. Yu, *Chem. Eur. J.,* 2010, **16**, 12000.
18 J. Liu, H. Xia, D. F. Xue, L. Lu, *J. Am. Chem. Soc.,* 2011, **133**, 20168.
19 G. Q. Zhang, W. Wang, Q. X. Yu, X. G. Li, *Chem. Mater.,* **2009**, ***21***, 969.
20 X. L. Dong, Z. Y. Guo, Y. F. Song, M. Y. Hou, J. Q. Wang, Y. G. Wang, Y. Y. Xia, *Adv. Funct. Mater.,* 2014, **24**, 3405.
21 Xu, Q. F. Wang, X. W. Wang, Q. Y. Xiang, B. Liang, D. Chen, G. Z. Shen, *ACS Nano,* 2013, **7**, 5453.
22 Z. Li, L. Zhang, B. S. Amirkhiz, X. H. Tan, Z. W. Xu, H. L. Wang, B. C. Olsen, C. M. B. Holt, D. Mitlin, *Adv. Energy Mater.,* 2012, **2**, 431.
23 H. Chen, L. F. Hu, Y. Yan, R. C. Che, M. Chen, L. M. Wu, *Adv. Energy Mater.,* 2013, **3**, 1636.
24 H. Jiang, C. Z. Li, T. Sun, Z. Ma, *Chem. Commun.,* 2012, **48**, 2606,
25 K. B. Xu, R. J. Zou, W. Y. Li, Y. F. Xue, G. S. Song, Q. Liu, X. J. Liu, J. Q. Hu, *J. Mater. Chem. A,* 2013, **1**, 9107.
26 R. R. Bi, X. L. Wu, F. F. Cao, L. Y. Jiang, Y. G. Guo, L. J. Wan, *J. Phys. Chem. C,* 2010, **114**, 2448.
27 L. J. Cao, S. B. Yang, W. Gao, Z. Liu, Y. J. Gong, L. L. Ma, G. Shi, S. D. Lei, Y. H. Zhang, S. T. Zhang, R. Vajtai, P. M. Ajayan, *Small,* 2013, **9**, 2905.
28 M. Jayalakshmi, M. M. Rao, *J. Power Sources,* 2006, **157**, 624.
29 Y. Wang, F. Y. Liu, Y. Ji, M. Yang, W. Liu, W. Wang, Q. S. Sun, Z. Q. Zhang, X. D. Zhao, X. Y. Liu, *Dalton Trans.,* 2015, **44**, 10431.
30 Z. C. Li, J. Han, L. Fan, R. Guo, *CrystEngComm,* 2015, **17**, 1952.
31 Q. H. Wang, L. F. Jiao, H. M. Du, Y. C. Si, Y. J. Wang, H. T. Duan, *J. Mater. Chem.,* 2012, **22**, 21387.
32 S. J. Peng, L. L. Li, H. T. Tan, R. Cai, W. H. Shi, C. C. Li, S. G. Mhaisalkar, M. Srinivasan, S. Ramakrishna, Q. Y. Yan, *Adv. Funct. Mater.,* 2014, **24**, 2155.
33 X. H. Xia, C. R. Zhu, J. S. Luo, Z. Y. Zeng, C. Guan, C. F. Ng, H. Zhang, H. J. Fan, *Small,* 2014, **10**, 766.
34 J. Q. Yang, X. C. Duan, Q. Qin, W. J. Zheng, *J. Mater. Chem. A,* 2013, **1**, 7880.
35 Y. Mu, D. L. Jia, Y. Y. He, Y. Q. Miao, H. L. Wu, *Biosens. Bioelectron.,* 2011, **26**, 2948.
36 S. Liu, J. Q. Tian, L. Wang, Y. L. Luo, W. B. Lu, X. P. Sun, *Biosens. Bioelectron.,* 2011, **26**, 4491.
37 Y. H. Ni, L. N. Jin, L. Zhang, J. M. Hong, *J. Mater. Chem.,* 2010, **20**, 6430.
38 H. Pang, Q. Y. Lu, J. J. Wang, Y. C. Li, F. Gao, *Chem. Commun.,* 2010, **46**, 2010.
39 S. Liu, B. Yu, T. Zhang, *Electrochim. Acta.,* 2013, **102**, 104.
40 C. Z. Wei, C. Cheng, J. H. Zhao, Y. Wang, Y. Y. Cheng, Y. Z. Xu, W. M. Du, H. Pang, *Chem. Asian J.,* 2015, **10**, 679.
41 J. Liu, D. F. Xue, *J. Mater. Chem.,* 2011, **21**, 223.
42 C. Y. Cao, W. Guo, Z. M. Cui, W. G. Song, W. Cai, *J. Mater. Chem.,* 2011, **21**, 3204.
43 C. Z. Wei, C. Cheng, B. B. Zhou, X. Yuan, T. T. Cui, S. S. Wang, M. B. Zheng, H. Pang, *Part. Part. Syst. Charact.,* 2015, **32**, 831.
44 X. Y. Yu, X. Z. Yao, T. Luo, Y. Jia, J. H. Liu, X. J. Huang, *ACS Appl. Mater. Interfaces.,* 2014, **6**, 3689.
45 C. Z. Wei, Q. Y. Lu, J. Sun, F. Gao, *Nanoscale,* 2013, **5**, 12224.
46 Y. Q. Fan, G. J. Shao, Z. P. Ma, G. L. Wang, H. B. Shao, S. Yan, *Part. Part. Syst. Charact.,* 2014, **31**, 1079.
47 C. Z. Yuan, X. G. Zhang, L. H. Su, B. Gao, L. F. Shen, *J. Mater. Chem.,* 2009, **19**, 5772.
48 N. N. Xiang, Y. H. Ni, X. Ma, *Chem. Asian J.*, 2015, DOI: 10.1002/asia.201500386.
49 G. Q. Zhang, X. W. Lou, *Sci. Rep*. 2013, **3**, 1470.
50 X. H. Wang, J. J. Ding, S. W. Yao, X. X. Wu, Q. Q. Feng, Z. H. Wang, B. Y. Geng, *J. Mater. Chem. A,* 2014, **2**, 15958.
51 C. Z. Yuan, L. H. Zhang, L. R. Hou, G. Pang, X. G. Zhang, *Part. Part. Syst. Charact.,* 2014, **31**, 778.
52 Y. Zhang, W. P. Sun, X. H. Rui, B. Li, H. T. Tan, G. L. Guo, S. Madhavi, Y. Zong, Q. Y. Yan, *Small,* 2015, **11**, 3720.
53 H. Z. Wan, J. J. Jiang, Y. J. Ruan, J. W. Yu, L. Zhang, H. C. Chen, L. Miao, S. W. Bie, *Part. Part. Syst. Charact.,* 2014, **31**, 857.
54 C. Z. Yuan, J. Y. Li, L. R. Hou, L. H. Zhang, X. G. Zhang, *Part. Part. Syst. Charact.,* 2014, **31**, 657.
55 X. H. Xia, D. L. Chao, Z. X. Fan, C. Guan, X. H. Cao, H. Zhang, H. J. Fan, *Nano Lett.,* 2014, **14**, 1651.
56 C. Z. Wei, C. Cheng, J. H. Zhao, Z. T. Wang, H. P. Wu, K. Y. Gu, W. M. Du, H. Pang, *ChemOpen,* 2015, **4**, 32.
57 D. G. Yang, P. C. Liu, Y. Gao, H. Wu, Y. Cao, Q. Z. Xiao, H. M. Li, *J. Mater. Chem.,* 2012, **22**, 7224.
58 Y. T. Zhang, L. Q. Luo, Z. Zhang, Y. P. Ding, S. Liu, D. M. Deng, H. B. Zhao, Y. G. Chen, *J. Mater. Chem. B,* 2014, **2**, 529.
59 F. Cao, S. Guo, H. Y. Ma, G. C. Yang, S. X. Yang, J. Geng, *Talanta,* 2011, **86**, 214.

View Article Online
DOI: 10.1039/C5DT02724A

60 P. Lu, Q. B. Liu, Y. Z. Xiong, Q. Wang, Y. T. Lei, S. J. Lu, L. W. Lu, L. Yao, *Electrochim. Acta.,* 2015, **168**, 148.
61 X. J. Zhang, A. X. Gu, G. F. Wang, Y. Huang, H. Q. Ji, B. Fang, *Analyst,* 2011, **136**, 5175.
62 C. Z. Wei, C. Cheng, J. H. Zhao, X. Yuan, T. T. Wu, Y. Wang, W. M. Du, H. Pang, *CrystEngComm,* 2015, **17**, 4540.
63 C. Z. Wei, Y. Y. Liu, X. R. Li, J. H. Zhao, Z. Ren, H. Pang, *ChemElectroChem,* 2014, **1**, 799.
64 J. X. Zhu, Z. Y. Yin, D. Yang, T. Sun, H. Yu, H. E. Hoster, H. H. Hng, H. Zhang, Q. Y. Yan, *Energy Environ. Sci.,* 2013, **6**, 987.
65 X. H. Kang, Z. B. Ma, X. Y. Zou, P. X. Cai, J. Y. Mo, *Anal. Biochem.,* 2007, **363**, 143.
66 M. C. Henstridge, E. F. Dickinson, M. Aslanoglu, C. B. McAuley, R. G. Compton, *Sens. Actuators, B,* 2010, **145**, 417.
67 I. Streeter, G. G. Wildgoose, S. L. Dong, R. G. Compton, *Sens. Actuators, B,* 2008, **133**, 462.
68 X. W. Li, S. L. Xiong, J. F. Li, J. Bai, Y. T. Qian, *J. Mater. Chem.,* 2012, **22**, 14276.
69 B. Wang, H. B. Wu, L. Yu, R. Xu, T. T. Lim, X. W. Lou, *Adv. Mater.,* 2012, **24**, 1111.

Table of Contents

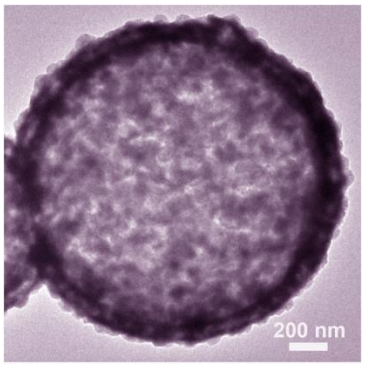

NiS_2 and α-NiS hollow spheres are successfully prepared via a template-free method. When evaluated NiS_2 and α-NiS hollow spheres for supercapacitors, glucose sensors and waste water treatment. It is found that the hollow α-NiS spheres exhibit better performance than that of the NiS_2 hollow sphere.